

Paradoxical roles of inhibitory autapse and excitatory synapse in formation of counterintuitive anticipated synchronization

Xue-Li Ding(丁学利), Hua-Guang Gu(古华光), Yu-Ye Li(李玉叶), and Yan-Bing Jia(贾雁兵)

Citation: Chin. Phys. B, 2023, 32 (**8**): 088701. DOI: 10.1088/1674-1056/acc450
Journal homepage: http://cpb.iphy.ac.cn; http://iopscience.iop.org/cpb

What follows is a list of articles you may be interested in

Effects of electric field on vibrational resonances in Hindmarsh-Rose neuronal systems for signal detection

Xiaoxia Li(李晓霞), Xiaopeng Xue(薛小鹏), Dongjie Liu(刘栋杰), Tianyi Yu(余天意), Qianqian He(何倩倩), and Guizhi Xu(徐桂芝)

Chin. Phys. B, 2023, 32 (**4**): 048701. DOI: 10.1088/1674-1056/ac9cc0

Effect of autaptic delay signal on spike-timing precision of single neuron

Xuan Ma(马璇), Yaya Zhao(赵鸭鸭), Yafeng Wang(王亚峰), Yueling Chen(陈月玲), and Hengtong Wang(王恒通)

Chin. Phys. B, 2023, 32 (**3**): 038703. DOI: 10.1088/1674-1056/ac7451

Pulse coding off-chip learning algorithm for memristive artificial neural network

Ming-Jian Guo(郭明健), Shu-Kai Duan(段书凯), and Li-Dan Wang(王丽丹)

Chin. Phys. B, 2022, 31 (**7**): 078702. DOI: 10.1088/1674-1056/ac4f4e

Relationship between manifold smoothness and adversarial vulnerability in deep learning with local errors

Zijian Jiang(蒋子健), Jianwen Zhou(周健文), and Haiping Huang(黄海平)

Chin. Phys. B, 2021, 30 (**4**): 048702. DOI: 10.1088/1674-1056/abd68e

Enhanced vibrational resonance in a single neuron with chemical autapse for signal detection

Zhiwei He(何志威), Chenggui Yao(姚成贵), Jianwei Shuai(帅建伟), and Tadashi Nakano

Chin. Phys. B, 2020, 29 (**12**): 128702. DOI: 10.1088/1674-1056/abb7f9

Paradoxical roles of inhibitory autapse and excitatory synapse in formation of counterintuitive anticipated synchronization

Xue-Li Ding(丁学利)[1], Hua-Guang Gu(古华光)[2,†], Yu-Ye Li(李玉叶)[3], and Yan-Bing Jia(贾雁兵)[4]

[1] *Department of Public Basic Education, Fuyang Institute of Technology, Fuyang* 236031, *China*
[2] *School of Aerospace Engineering and Applied Mechanics, Tongji University, Shanghai* 200092, *China*
[3] *College of Mathematics and Computer Science, Chifeng University, Chifeng* 024000, *China*
[4] *School of Mathematics and Statistics, Henan University of Science and Technology, Luoyang* 471000, *China*

(Received 8 January 2023; revised manuscript received 7 March 2023; accepted manuscript online 15 March 2023)

Different from the common delayed synchronization (DS) in which response appears after stimulation, anticipated synchronization (AS) in unidirectionally coupled neurons denotes a counterintuitive phenomenon in which response of the receiver neuron appears before stimulation of the sender neuron, showing an interesting function of brain to anticipate the future. The dynamical mechanism for the AS remains unclear due to complex dynamics of inhibitory and excitatory modulations. In this article, the paradoxical roles of excitatory synapse and inhibitory autapse in the formation of AS are acquired. Firstly, in addition to the common roles such that inhibitory modulation delays and excitatory modulation advances spike, paradoxical roles of excitatory stimulation to delay spike via type-Ⅱ phase response and of inhibitory autapse to advance spike are obtained in suitable parameter regions, extending the dynamics and functions of the excitatory and inhibitory modulations. Secondly, AS is related to the paradoxical roles of the excitatory and inhibitory modulations, presenting deep understandings to the AS. Inhibitory autapse induces spike of the receiver neuron advanced to appear before that of the sender neuron at first, and then excitatory synapse plays a delay role to prevent the spike further advanced, resulting in the AS as the advance and delay effects realize a dynamic balance. Lastly, inhibitory autapse with strong advance, middle advance, and weak advance and delay effects induce phase drift (spike of the receiver neuron advances continuously), AS, and DS, respectively, presenting comprehensive relationships between AS and other behaviors. The results present potential measures to modulate AS related to brain function.

Keywords: anticipated synchronization, inhibitory autapse, excitatory synapse, paradoxical firing

PACS: 87.18.Sn, 87.19.lm **DOI:** 10.1088/1674-1056/acc450

1. Introduction

Synchronization is ubiquitous in the nervous systems, such as complete synchronization, in-phase synchronization, anti-phase synchronization, delayed synchronization, and anticipated synchronization. The synchronization in the nervous system is associated with information processing, locomotor, cognitive function, and even brain diseases such as the epilepsy.[1,2] In unidirectionally coupled sender and receiver systems, response of a receiver system always appears after the stimulation of the sender system, which is the well-known delay synchronization (DS). The DS is a very common phenomenon consistent with our general view. If a self-feedback with time delay is introduced to the receiver system, the response of the receiver system occurs before the stimulation of the sender system, which is called the anticipated synchronization (AS, more details please refer to Appendix A of this article).[3–5] The AS has been widely studied in many nonlinear systems, presenting counterintuitive behavior different from the DS.[6–10]

AS has been extended to the nervous system in both theoretical models and experiments.[11–22] The AS in the coupled neurons means that the response spike of the receiver neuron appears before the stimulation spike of the sender neuron, implying that the nervous system may anticipate the future, which is a very interesting phenomenon for the brain function. The AS in the nervous is studied in two unidirectionally coupled FitzHugh–Nagumo neuron models[11] with time delay, and then studied in the coupled Hindmarsh–Rose models[12] and coupled Rulkov models.[13] Recently, feedback delays can enhance anticipatory synchronization in human-machine interaction,[14] and delayed feedback embedded in perception-action coordination cycles results in anticipation behavior during synchronized rhythmic action (two-person alternating rhythm-clapping in the presence of a range of constant auditory transmission latency).[15] Both experimental results are explained with AS in the system with delay. Without time delay, AS can be simulated in coupled Hodgkin–Huxley (HH) models.[16] In the sender-receiver HH neuron models via one-way excitatory synaptic coupling, DS appears. If an inhibitory interneuron with delayed negative feedback is introduced to the receiver neuron to form a system composed of three neurons, AS is induced in suitable parameter ranges.[16] Recently, AS is simulated in the neuronal networks with both inhibitory and excitatory synaptic couplings,[17,23,24] which presents alternative explanation to the AS in local field potentials recorded from different brain

†Corresponding author. E-mail: guhuaguang@tongji.edu.cn
© 2023 Chinese Physical Society and IOP Publishing Ltd

regions of monkey.[25,26] In addition, the song of bird[27] and visually guided movement[28] are also suggested to be related to the AS. Furthermore, AS is demonstrated in electroencephalogram (EEG) signal and in human.[29] EEG is recorded synchronously from different brain regions when motor and conscious responses to visual stimulation are tested. With granger causality analysis, the information flow is acquired to be from the posterior parietal cortex (sender) to the primary motor cortex and the primary somatosensory cortex (receiver). However, with the spectrum analysis, the EEG of the posterior parietal cortex occurs before that of the primary motor cortex and the primary somatosensory cortex, due to the fact that the dominant frequency of the EEG has a negative phase difference. For the AS observed in different brain regions of monkey and human, the possible functions of AS in cognitive processing or learning are discussed.[17,25] In a recent study, DS of a sender-receiver Izhikevich neuronal system with a unidirectional excitatory coupling changes to AS when an autapse with suitable parameters is introduced to the receiver neuron.[18] Then, the inhibitory autaptic current and the excitatory synaptic current induce the spike of the receiver neuron advanced to appear before the spike of the sender neuron at first, and then, the two currents can realize a dynamic balance to ensure the fixed interspike intervals (ISIs) of the receiver neuron to form the stable AS. Identification of the roles of two currents in advancing or delaying the spike of the receiver neuron is most important to recognize the dynamical mechanism of the counterintuitive anticipated synchronization.

In fact, it is well-known that the inhibitory modulation plays a common role to suppress firing activity, for example, delay a spike, and the excitatory modulation plays a common role to enhance firing, for instance, advance a spike. The balance between the excitatory and inhibitory modulations is the guarantee to the normal brain function, and the imbalance between the excitation/inhibition modulations is always related to brain diseases. However, recently, various examples in contrast to the common viewpoint on the roles of the inhibitory and excitatory modulations are observed in both single neurons and neuronal networks.[30–39] Such counterintuitive or paradoxical roles of the excitatory or inhibitory modulations have attracted much attention in both theoretical and experimental studies.[33–36] For example, inhibitory stimulation can induce a spike from the quiescent state, called post-inhibitory rebound spike, which is related to the major depressive disorder or parkinson diseases in recent experiments.[40,41] In addition, the paradoxical role of the excitatory modulation is also studied.[36,42,43] For the spiking with the type-Ⅱ phase response curve (PRC), an excitatory stimulation pulse with a small application phase can play a counterintuitive role to delay the next spike to reduce the spiking activity. The excitatory modulation to spiking with type-I PRC plays a common role. Unfortunately, the common or paradoxical role (type I or Ⅱ PRC) of the excitatory synaptic current on spiking of the Izhikevich neuronal model in the formation of AS has not been studied.

Recently, the paradoxical role of the autapse (a special synapse connecting to the neuron itself widely observed in multiple types of neuron) has attracted much attention,[44–58] in addition to its common role in modulating electrical behaviors of single neurons and neuronal networks have been studied.[44–53] For example, inhibitory autapse has been observed in inhibitory interneurons. In addition to the common role to inhibit the firing activity, which is observed in the hippocampus and neocortex,[54] inhibitory autapse is identified to play counterintuitive role to enhance firing. For example, inhibitory autapse can evoke spiking from the quiescent state, i.e., post-inhibitory rebound spiking.[55] When time delay is considered, the inhibitory autapse can play a paradoxical role to enhance spiking in a theoretical model.[36] However, in the absence of time delay, the role of the inhibitory autapse on spiking activity of the Izhikevich model has attracted little attention. In addition, the dynamical mechanism for the DS and phase-drift (PD) behaviors appearing around the AS remains unclear.

Then, the roles of inhibitory autaptic current and excitatory synaptic current in the formation of the AS, DS, and PD are studied in this article. Firstly, the inhibitory autapse to the Izhikevich model is identified to play paradoxical role to advance the spike of spiking in a wide parameter region, which can be further distinguished into strong, middle, and weak advance effects. The Izhikevich model exhibits type-Ⅱ PRC, showing that the excitatory stimulation with a small application phase plays a paradoxical role to delay the spike. The results present a novel example of the paradoxical phenomenon of the inhibitory autapse and excitatory stimulation in the Izhikevich model. Secondly, both the inhibitory autaptic current and excitatory synaptic current play paradoxical roles in the formation of the AS. The inhibitory autaptic current induces the spike of the receiver neuron advanced to appear before the spike of the sender neuron, and then the excitatory current plays a delay role to prevent the spike further advanced. As the two opposite effects realize a dynamic balance, the stable AS forms. Then, the counterintuitive phenomenon of the coupled neurons is built in relationships to the paradoxical roles of inhibitory and excitatory modulations on single neurons. Lastly, the AS is distinguished with other dynamical behaviors of DS and PD. As the advance effect of inhibitory autapse is strong to be dominant, the spike of the receiver neuron always advances, which is the PD behavior. The DS appears when the delay effect of the excitatory synaptic current is dominant. The results present an essential dynamical mechanism for the AS and the relationships among the AS, DS, and PD, which are helpful for modulating the AS.

The rest of this article is organized as follows. Section 2 presents the model and methods. The result is addressed in Section 3. Finally, we present the conclusions in Section 4.

2. Model and methods

2.1. Model of sender neuron and receiver neuron with autapse

It is well known that the information transmission of the chemical synapse instead of electrical synapse is unidirectional. In this work, the typical sender-receiver configuration consists of two unidirectionally coupled neurons with an excitatory synapse (small solid triangle), as shown in Fig. 1. One is the sender neuron (labeled as S) and the other is the receiver neuron (labeled as R). The neuron R receives the excitatory synaptic current ($I_{\rm E}$) from the neuron S. Both neurons are described by the Izhikevich model. An inhibitory autapse (blue circle) is introduced to the receiver neuron (R), and then the model of the sender neuron and the receiver neuron with autapse is formed.

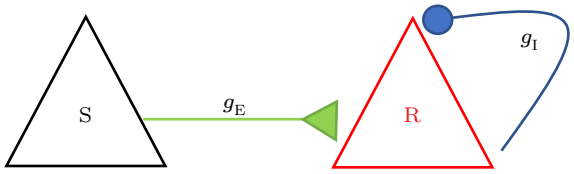


Fig. 1. The receiver neuron R receives the excitatory synaptic current (small triangle represents with the conductance $g_{\rm E}$) from the sender neuron S and the inhibitory autaptic current (the circle denotes with the conductance $g_{\rm I}$) from itself.

The model is described by the following equations:[18,59]

$$\frac{{\rm d}V_{\rm S}}{{\rm d}t} = 0.04V_{\rm S}^2 + 5V_{\rm S} + 140 - U_{\rm S} + I_{\rm app}, \tag{1}$$

$$\frac{{\rm d}U_{\rm S}}{{\rm d}t} = a(bV_{\rm S} - U_{\rm S}), \tag{2}$$

$$\frac{{\rm d}V_{\rm R}}{{\rm d}t} = 0.04V_{\rm R}^2 + 5V_{\rm R} + 140 - U_{\rm R} + I_{\rm app} + I_{\rm E} + I_{\rm I}, \tag{3}$$

$$\frac{{\rm d}U_{\rm R}}{{\rm d}t} = a(bV_{\rm R} - U_{\rm R}), \tag{4}$$

where the variable $V_{\rm S}$ and $U_{\rm S}$ denote the membrane potential and recovery variable of neuron S, $V_{\rm R}$ and $U_{\rm R}$ denote the membrane potential and recovery variable of neuron R. $I_{\rm app}$ is an external current. The reset condition is given as follows: if $V \geq 30$ mV, then $V \leftarrow c$ and $U \leftarrow U + d$ ($c = -65$, $d = 8$).

The excitatory synaptic current from the neuron S to R is $I_{\rm E} = g_{\rm E} r_{\rm E}(E_{\rm E} - V_{\rm R})$, where $g_{\rm E}$ is conductance of the excitatory synapse, $E_{\rm E}$ is the reversal potential of the excitatory synapse, and $r_{\rm E}$ represents the gating variable to describe the fraction of open synaptic channels. $I_{\rm I} = g_{\rm I} r_{\rm I}(E_{\rm I} - V_{\rm R})$ is the inhibitory autaptic current, where $g_{\rm I}$ is conductance of the inhibitory autapse, and $E_{\rm I}$ is the corresponding reversal potential. The variable $r_{\rm I}$ denotes the gating variable to describe the fraction of open synaptic channels. The first-order kinetic model of $r_{\rm E}$ and $r_{\rm I}$ is expressed as follows:

$$\frac{{\rm d}r_{\rm E}}{{\rm d}t} = \alpha_{\rm E}[T_{\rm E}](1 - r_{\rm E}) - \beta_{\rm E} r_{\rm E}, \tag{5}$$

$$\frac{{\rm d}r_{\rm I}}{{\rm d}t} = \alpha_{\rm I}[T_{\rm I}](1 - r_{\rm I}) - \beta_{\rm I} r_{\rm I}, \tag{6}$$

where $[T_{\rm E}]$ represents the neurotransmitter concentration, which is a sigmoid function of the presynaptic potential $V_{\rm pre}$, i.e., $[T_{\rm E}] = \frac{T_{\max}}{1+{\rm e}^{[-(V_{\rm pre}-V_{\rm p})/K_{\rm p}]}}$. $V_{\rm pre} = V_{\rm S}$ for the excitatory synapse, and $\alpha_{\rm E}$ and $\beta_{\rm E}$ are the rise and decay rate constants, respectively. $[T_{\rm I}] = \frac{T_{\max}}{1+{\rm e}^{[-(V_{\rm pre}-V_{\rm p})/K_{\rm p}]}}$, and $V_{\rm pre} = V_{\rm R}$ for an autapse. Here, $\alpha_{\rm I}$ and $\beta_{\rm I}$ are the rise and decay rate, respectively. $T_{\max}$ is the maximum value of $[T_{\rm I}]$, $K_{\rm p}$ is the steepness, and $V_{\rm R}$ is half-activated value of $[T_{\rm I}]$.

The parameter values are set as follows:[18,59] $a = 0.02$, $b = 0.2$, $T_{\max} = 1$ mM, $K_{\rm p} = 5$ mV, $V_{\rm p} = 2$ mV, $E_{\rm E} = 35$ mV, $\alpha_{\rm E} = 1.1$ mM^{-1}·ms^{-1}, $E_{\rm I} = -80$ mV, and $\alpha_{\rm I} = 5$ mM^{-1}·ms^{-1}. $g_{\rm E}$, $\beta_{\rm E}$, $g_{\rm I}$, and $\beta_{\rm I}$ are chosen as the control parameters.

2.2. Methods

The equations are solved by the fourth-order Runge–Kutta method and an integration step of 0.001 ms is used.

3. Results

3.1. Paradoxical roles of the excitatory stimulation and inhibitory autapse on a single neuron

In this subsection, only a single neuron, i.e., neuron R with $I_{\rm E} = 0$, is studied. Then, the $V_{\rm R}$ is labeled as V because only a single neuron is considered.

3.1.1. Type-Ⅱ PRC showing paradoxical roles of excitatory modulation with a small phase

Spiking responses of the Izhikevich model without inhibitory autapse to an excitatory pulse current stimulation are studied firstly. Then, Eqs. (3) and (4) with $I_{\rm E} = 0$ and $I_{\rm I} = 0$ are studied.

The spiking exhibits type-Ⅱ PRC to excitatory stimulation. Two spikes of spiking behavior for $I_{\rm app} = 10$ μA·cm^{-2} are shown by the solid black curve in Fig. 2(a), and the period (i.e., the time interval between two spikes) is T_0 ($T_0 \approx 44.813$ ms). When an excitatory pulse (violet curve) is applied at $t_{\rm s}$ after the former spike, the spike following the stimulation changes to appear at T_1 after the former spike. A normalized phase θ is defined as

$$\theta(t_{\rm s}) = (T_0 - T_1)/T_0. \tag{7}$$

Here, θ can be used to characterize the phase response of the spiking. For a stimulation pulse with amplitude $I_{\rm s} = 0.5$ μA·cm^{-2} and duration $D_{\rm s} = 1$ ms applied at $t_{\rm s} = 35$ ms, $T_1 \approx 44.416$ ms, as shown in Fig. 2(a). T_1 is smaller than T_0,

then $\theta(35) \approx 0.0089 > 0$, showing that the spike (red) following the stimulation advances. The parameters used to describe the dynamics of single neuron or coupled neurons are given in Appendix B.

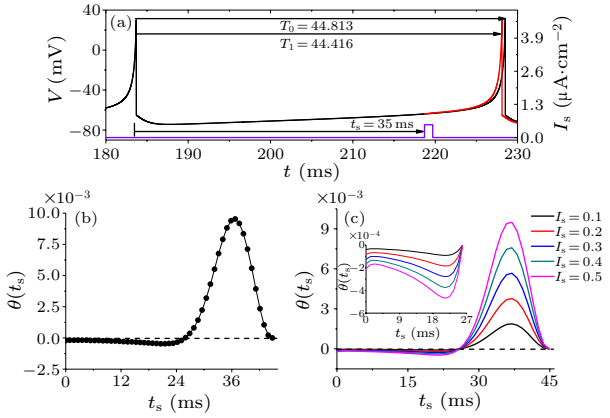


Fig. 2. Type-Ⅱ PRC of spiking for $I_{app} = 10$ μA· cm^{-2}. (a) A positive pulse stimulation with amplitude $I_s = 0.5$ μA·cm^{-2} and width $D_s = 1$ ms (violet curve) applied at $t_s = 35$ ms after the former spike (black). (b) PRC [$\theta(t_s)$ versus t_s] for $I_s = 0.5$ μA·cm^{-2} and $D_s = 1$ ms. (c) PRCs for different strengths I_s. Inset: Enlargement for small t_s values.

The values of $\theta(t_s)$ at different values of t_s are acquired as the PRC, as depicted in Fig. 2(b). When t_s is small and middle (shorter than ~ 26 ms), $\theta(t_s)$ is negative, which corresponds to delayed spike. The delay effect presents a paradoxical role of the excitatory stimulation with a small application phase. When t_s is large (longer than ~ 26 ms), $\theta(t_s)$ is positive, showing that spike advances, which corresponds to a common role. Such a PRC with both negative and positive responses shows that the Izhikevich neuron model manifests type-Ⅱ PRC. The PRC curves at different stimulation strengths are all type Ⅱ, as shown in Fig. 2(c). For a small t_s value, the stronger the excitatory stimulation is, the stronger the delay effect is.

3.1.2. Paradoxical roles of inhibitory autapse in a wide parameter range

The influences of inhibitory autapse on single Izhikevich neuron without excitatory stimulation [Eqs. (3) and (4) with $I_E = 0$] are studied.

For a single neuron, the inhibitory autapse can induce spike advanced (i.e., ISI reduced) in wide ranges of g_I and β_I and is delayed in the remaining ranges. For example, for $g_I = 3$ μS/cm^2 and $\beta_I = 0.2$ ms^{-1}, the solid red curve represents the membrane potential modulated by the inhibitory autapse, and the dashed black denotes the spike trains without the autapse, as shown in Fig. 3(a). The spikes (red) modulated by the inhibitory autapse advance, resulting in shortened ISIs (i.e., enhanced firing activity). The shortened ISIs presents a paradoxical phenomenon in contrast to the general view that inhibitory modulations should suppress firing activity. The blue curve in Fig. 3(a) represents the autaptic current, which plays a role to advance the spike. However, for the autapse with $g_I = 2$ μS/cm^2 and $\beta_I = 0.1$ ms^{-1}, spikes (red) delay and ISIs become longer, compared with those without autapse (dashed black curve), as illustrated in Fig. 3(b). The result shows a common phenomenon for the inhibitory autapse. The blue curve represents the autaptic current, which delays the spikes.

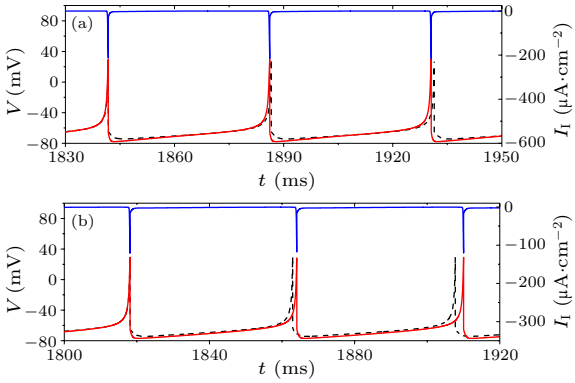


Fig. 3. Changes of spikes and autaptic current (blue) of a single neuron after introducing the inhibitory autapse with different parameter values. (a) Advanced spikes (i.e., shortened ISIs) for $g_I = 3$ μS/cm^2 and $\beta_I = 0.2$ ms^{-1}. (b) Delayed spikes (i.e., lengthened ISIs) for $g_I = 2$ μS/cm^2 and $\beta_I = 0.1$ ms^{-1}. The dashed black and solid red curves denote the spike trains without and with autapse, respectively. $I_{app} = 10$ μA·cm^{-2}.

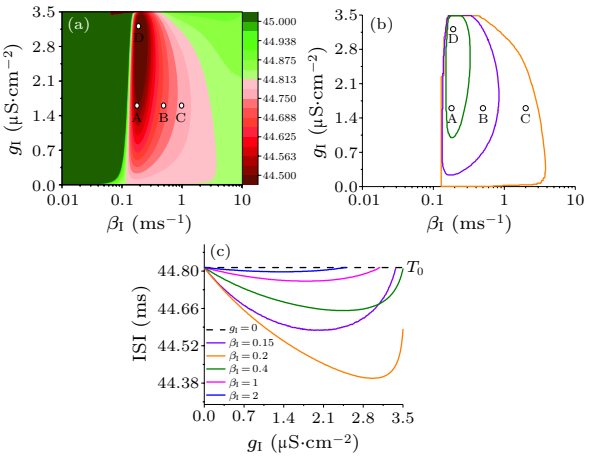


Fig. 4. Advance effect characterized by shortened ISIs induced by the inhibitory autapse. (a) The detailed values of ISIs in the plane (β_I, g_I). Black/red and green represent shortened ISIs and lengthened ISIs, respectively. Black, deep red, and light red denote the strong, middle, and weak advance effects. Points A, B, and C are representative of the strong, middle, and weak advance effects, and point D locates within the region of the strongest advance effect. (b) Olive, violet, and orange curves represent the border of strong, middle, and weak advance effect regions, respectively. (c) Changes of shorted ISIs with respect to g_I at $\beta_I = 0.15$ ms^{-1} (violet), 0.2 ms^{-1} (orange), 0.4 ms^{-1} (olive), 1 ms^{-1} (magenta), and 2 ms^{-1} (blue). The dashed black line represents the ISI value (T_0) in the absence of inhibitory autapse. $I_{app} = 10$ μA·cm^{-2}.

The detailed values of ISIs on the plane (β_I, g_I) are shown in Fig. 4(a) ($I_{app} = 10$ μA·cm^{-2}). The stronger the black or red is, the shorter the ISI is, i.e., the stronger the advance effect is. The stronger the green is, the longer the ISI is, i.e., the stronger the delay effect is. The advance effect of the inhibitory autapse is strong, middle, and weak within the black, deep red, and light red areas, respectively. For example, the inhibitory autapses for points A ($\beta_I = 0.18$ ms^{-1}, $g_I = 1.6$ μS/cm^2),

B ($\beta_{\rm I} = 0.5$ ms^{-1}, $g_{\rm I} = 1.6$ μS/cm^2), and C ($\beta_{\rm I} = 1$ ms^{-1}, $g_{\rm I} = 1.6$ μS/cm^2) in Fig. 4(a) exhibit strong, middle, and small advance effects, respectively. The neighborhood around point D ($\beta_{\rm I} = 0.19$ ms^{-1}, $g_{\rm I} = 3.21$ μS/cm^2) within the black region exhibits the strongest advance effect, corresponding to the minimal ISIs. As shown in Fig. 4(b), the olive, violet, and orange curves denote the borders of the strong advance effect, middle advance effect, and weak advance effect regions, respectively.

The changes of ISIs with respect to $g_{\rm I}$ at different values of $\beta_{\rm I}$ are depicted in Fig. 4(c), wherein the dashed horizontal line represents $T_0 \approx 44.813$ ms which corresponds to the ISI value in the absence of inhibitory autapse ($\beta_{\rm I} = 0$ ms^{-1}). For a fixed $\beta_{\rm I}$, ISI of spiking decreases firstly and then increases with increasing $g_{\rm I}$. With increasing $\beta_{\rm I}$, the level of ISIs increases at first [from $\beta_{\rm I} = 0.15$ ms^{-1} (violet) to 0.2 ms^{-1} (orange)] and then gradually decreases [$\beta_{\rm I} = 0.15$ ms^{-1} (violet) and 1 ms^{-1} (magenta)] in the most ranges of $g_{\rm I}$, whereas the range of $g_{\rm I}$ becomes narrower. The shorter the ISI is, the stronger the advance effect is.

3.2. Representative of DS, AS, and PD in the coupled neurons

3.2.1. DS of coupled neurons with solely excitatory synapse (without autapse)

The DS behaviors of the coupled neurons with solely excitatory synapse (without autapse) are investigated as the control. Then, Eqs. (1)–(4) with $I_{\rm I} = 0$ are studied.

At $t = 0$ ms, the spike of neuron S (black) is assigned to be prior to that (red) of neuron R, and the interval between the first spikes of two neurons is relatively large. Then, the excitatory synapse from neuron S to neuron R plays a role at $t > 0$ ms. Without loss of generality, excitatory synapse with $g_{\rm E} = 0.3$ μS/cm^2 and $\beta_{\rm E} = 0.3$ ms^{-1} is considered as a representative. The evolutions from the transient behavior to the stable DS behavior are shown in Fig. 5(a). The membrane potentials of neurons S and R are depicted by the black and red curves, respectively. The interval between the i-th spikes of neurons S and R is defined as $\tau_i = t_i^{\rm R} - t_i^{\rm S}$, where i represents the sequential number of the spikes, and $t_i^{\rm S}$ and $t_i^{\rm R}$ are the peak times of the i-th spikes of neurons S and R, respectively. With increasing i, if $\tau_i = t_i^{\rm R} - t_i^{\rm S}$ converges to a constant positive value, labeled as $\tau_{\rm s}$ ($\tau_{\rm s} \approx 1.308$), the stable DS occurs, as illustrated in Fig. 5(b). The lower and upper x-axes denote the sequential number i and the time t, respectively. For the stable DS, the i-th spike of the neuron S (black) is prior to the i-th spike of the neuron R (red).

The distribution of $\tau_{\rm s}$ on the plane ($\beta_{\rm E}$, $g_{\rm E}$) is depicted in Fig. 5(c). Complex firing appears at the red-yellow area (middle left), due to the slow dynamics of the synaptic current (i.e., $\beta_{\rm E}$ is small). No black ($\tau_{\rm s} < 0$) appears in the remaining area, showing that the DS appears and non-AS appears for the excitatory synapse.

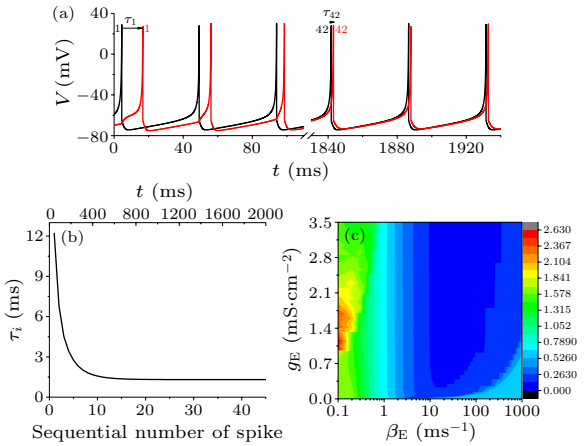


Fig. 5. DS behavior in the coupled neurons with solely excitatory synapse and without autapse. (a) The process from a transient behavior to the stable DS ($g_{\rm E} = 0.3$ μS/cm^2 and $\beta_{\rm E} = 0.3$ ms^{-1}). The black and red curves represent the membrane potentials of neurons S and R, respectively. The black and red numbers denote the sequential numbers of spikes of neurons S and R, respectively. (b) The change of time interval τ_i with respect to the time t (top x-axis) and i (bottom x-axis) corresponding to panel (a). (c) The distribution of $\tau_{\rm s}$ on the plane ($\beta_{\rm E}$, $g_{\rm E}$).

3.2.2. AS for middle advance effect of inhibitory autapse

The AS behavior of the coupled neurons with both excitatory synapse and inhibitory autapse is investigated. Then, Eqs. (1)–(4) are studied.

After an inhibitory autapse with advance effect is introduced to the neuron R, the coupled neurons can generate AS, PD or DS behaviors, which are dependent on the degree of advance effect of the inhibitory autapse. For example, in the absence of the inhibitory autapse, DS with $\tau_{\rm s} \approx 1.332$ ms appears for $g_{\rm E} = 0.1$ μS/cm^2 and $\beta_{\rm E} = 0.3$ ms^{-1}.

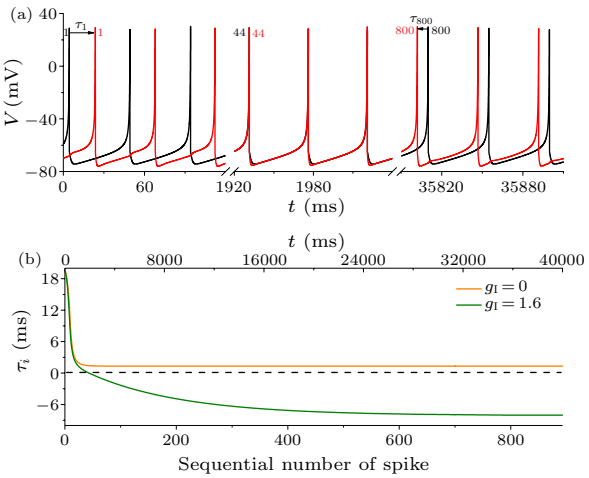


Fig. 6. AS modulated by inhibitory autapse for $g_{\rm E} = 0.1$ μS/cm^2 and $\beta_{\rm E} = 0.3$ ms^{-1}. (a) Evolution process of membrane potentials of neurons S (black) and R (red) from transient behavior to stable AS behavior for $g_{\rm I} = 1.6$ μS/cm^2. (b) The change of τ_i with respect to i (lower x-axis) and time t (upper x-axis) for the AS induced by inhibitory autapse (olive) and for the DS in the absence of inhibitory autapse (orange).

After introducing the inhibitory autapse corresponding to point B (middle advance effect), point A (strong advance ef-

fect), and point C (weak advance effect) in Fig. 4(a) to the neuron R, we can see that AS (Figs. 6 and 7), PD (Fig. 8), and DS (Fig. 9) appear.

The evolution process from transient behavior to stable AS for $g_{\rm E} = 0.1$ μS/cm^2 and $\beta_{\rm E} = 0.3$ ms^{-1}, and $g_{\rm I} = 1.6$ μS/cm^2 and $\beta_{\rm I} = 0.5$ ms^{-1} can be divided into 3 segments, as shown in Fig. 6(a), and the change of $\tau_i = t_i^{\rm R} - t_i^{\rm S}$ is shown by the olive curve in Fig. 6(b). The first segment (before $\sim$ 1894 ms) corresponds to transient behavior with $\tau_i > 0$ ($i < 43$, and the 43$^{\rm th}$ spike appearing at 1886 ms), similar to the DS to a certain extent. The second segment corresponds to transient behavior from $\sim$ 1894 ms to $\sim$ 35500 ms ($44 \le i \le 793$), and $\tau_i = t_i^{\rm R} - t_i^{\rm S}$ becomes negative first and then becomes more negative gradually. Different from the first segment, the i-th ($44 \le i \le 793$) spike of neuron R appears before the i-th spike of neuron S. During the last segment ($>$ 35500 ms), negative τ_i remains unchanged, resulting in the stable AS. The unchanged value of τ_i is labeled as $\tau_{\rm s}$ and $\tau_{\rm s} \approx -8.026$ ms (lower than zero, represented by the horizontal line). Obviously, the AS with $\tau_{\rm s} \approx -8.026$ ms is different from the DS with $\tau_{\rm s} \approx 1.332$ ms (orange) for the solely excitatory synapse with $g_{\rm E} = 0.1$ μS/cm^2 and $\beta_{\rm E} = 0.3$ ms^{-1}, as depicted in Fig. 6(b).

3.2.3. Dynamical mechanism for the AS

For the stable AS behavior shown in Fig. 7(a), neuron R receives the autaptic current (blue) and the excitatory synaptic current (magenta). The spike trains of neuron S and neuron R are denoted by the black curve and the red curve, respectively. Obviously, the autaptic current plays a role to advance the spike, as indicated in Fig. 3(a). The excitatory current (magenta) activated by the i-th spike of neuron S influences the (i+1)-th spike of neuron R, as shown in Fig. 7(a). For example, the excitatory synaptic current from the 801-th spike of neuron S plays a role at phase $t_{\rm s_801}$ after the 801-th spike of neuron R, which influences the timing of the 802-th spike of neuron R. The application phase $t_{\rm s_801}$ equals $-\tau_{801}$ (τ_{801} is negative); $\tau_{801} = \tau_{\rm s} = -8.026$ ms. Then, $t_{\rm s_801} = 8.026$ ms, which is shorter than 26 ms in Fig. 2(c). According to the PRC shown in Fig. 2(c), the excitatory synaptic current from 801-th spike of neuron S should play a paradoxical role to delay the 802-th spike of neuron R, due to a small application phase of the excitatory synaptic current.

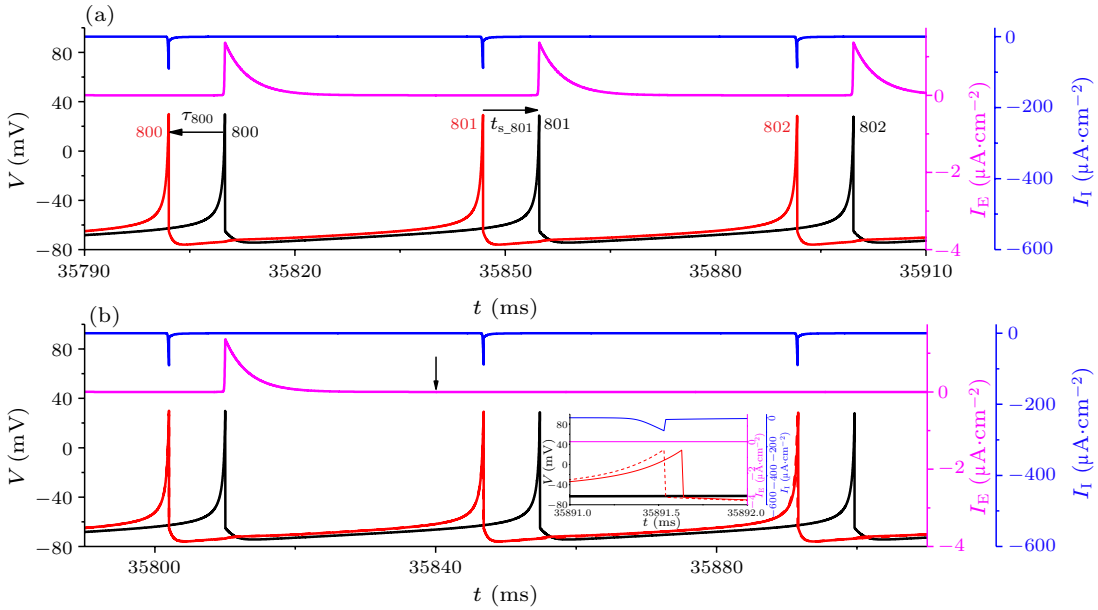


Fig. 7. Roles of the inhibitory autaptic current (blue) and the excitatory synaptic current (magenta) in the formation of stable AS (red and black represent the spike trains of neurons R and S, respectively). (a) A dynamic balance between the inhibitory autaptic current (blue) and the excitatory synaptic for the AS. (b) The delay effect of the excitatory synaptic current (magenta). The excitatory synapse is terminated ($g_{\rm E} = 0$ μS/cm^2) at a time ($t = 35840$ ms labeled by an down black arrow) before 801-th spike, and then the 802-th spike of neuron R (dashed red curve) advances, compared with the 802-th spike (solid red curve) of neuron R for $g_{\rm E} = 0.1$ μS/cm^2. Inset represents the local enlargement of the 802-th spikes for $g_{\rm E} = 0$ μS/cm^2 and $g_{\rm E} = 0.1$ μS/cm^2.

The delay effect of the excitatory synaptic current can be verified by the comparison to the response of neuron R when the excitatory synaptic current is terminated, as shown in Fig. 7(b). If the strength of the excitatory synapse is decreased from $g_{\rm E} = 0.1$ μS/cm^2 to $g_{\rm E} = 0$ μS/cm^2 ($t > 35840$ ms) before the 801-th spike of neuron R, then the excitatory synaptic current after the 801-th spike becomes zero, as shown by magenta in Fig. 7(b). Then, the 802-th spike (dashed red curve) of neuron R for $g_{\rm E} = 0$ μS/cm^2 advances, compared with that of $g_{\rm E} = 0.1$ μS/cm^2 [solid red curve in Fig. 7(b)]. The inset within Fig. 7(b) is the enlargement of the 802-th spikes, wherein the dashed red curve is for $g_{\rm E} = 0$ μS/cm^2 and the solid red curve is for $g_{\rm E} = 0.1$ μS/cm^2. The result shows that the excitatory synaptic current plays a role to delay the spike of neuron R, like the excitatory stimulation with a small application phase shown in Fig. 2(c). For the stable AS, the advance

effect of the inhibitory autaptic current (blue) and the delay effect of the excitatory synaptic current (magenta) can realize a dynamic balance. Then, modulated by these two currents, the period of spiking of neuron R is still T_0, which is the same as that without modulation. The result shows that the comprehensive effect of the two currents on the period of spiking of neuron R is zero, i.e., a dynamic balance between the two currents.

In addition, it should be noticed that the larger the excitatory synaptic conductance $g_{\rm E}$ is, the larger the excitatory synaptic current is, and the stronger the delay effect of the excitatory synaptic current is.

3.2.4. PD appearing for strong advance effect of the inhibitory autapse

For the DS without inhibitory autapse ($g_{\rm E} = 0.1$ μS/cm^2 and $\beta_{\rm E} = 0.3$ ms^{-1}), after the inhibitory autapse with strong advance effect ($g_{\rm I} = 1.6$ μS/cm^2 and $\beta_{\rm I} = 0.18$ ms^{-1}) is introduced, the PD is evoked, as shown in Fig. 8. For the PD behavior, the advance effect of the inhibitory autapse is strong enough to overcome the delay effect of the excitatory synaptic current, and the excitatory synaptic and inhibitory autaptic currents cannot realize a dynamic balance. Then, the spikes of neuron R always advance, modulated dominantly by the inhibitory autapse. With increasing i, τ_i does not converge to a fixed value but becomes more negative continuously and gradually, as depicted by the olive curve in Fig. 8(b), different from the orange curve which represents the positive τ_i of the DS in the absence of inhibitory autapse ($g_{\rm I} = 0$ μS/cm^2). The spike of neuron R always advances, as shown in Fig. 8(a). At the beginning, the i-th spike of neuron R appears after the i-th spike of neuron S. For $t \approx 990$–6995 ms, the i-th spike of neuron R appears before the i-th spike of neuron S. For $t \approx 6995$–13000 ms, the $(i+1)$-th spike of neuron R appears before the i-th spike of neuron S. For $t \approx 13000$–19005 ms, the $(i+2)$-th spike of neuron R appears before the i-th spike of neuron S. Then, the change of τ_i exhibits different segments divided by the dashed vertical lines in Fig. 8(b), and the different segments are labeled with 0, 1, 2, and 3. For the segment 0, τ_i decreases from a positive value to zero at $t \approx 960$ ms, which appears before the first vertical dashed line. For the segment labeled with k ($k = 1$, 2, and 3, ...), the $(i+k-1)$-th spike of neuron R appears before the i-th spike of neuron S. The results for $k > 3$ are not shown here.

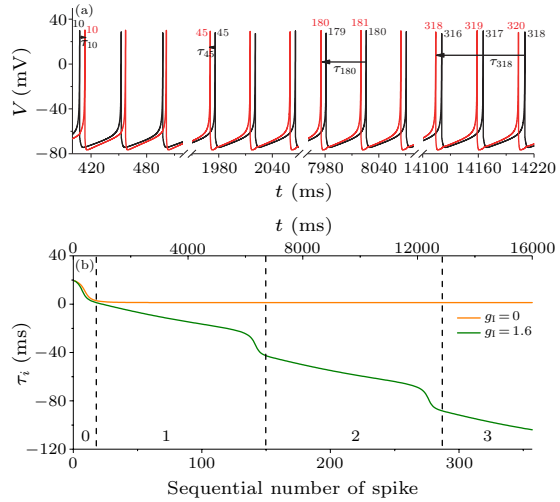


Fig. 8. Phase drift (PD) for $g_{\rm E} = 0.1$ μS/cm^2 and $\beta_{\rm E} = 0.3$ ms^{-1}, and $g_{\rm I} = 1.6$ μS/cm^2 and $\beta_{\rm I} = 0.18$ ms^{-1}. (a) Membrane potentials of neurons S (black) and R (red). The numbers represent the sequential numbers of spikes. (b) The change of τ_i with respect to i (lower x-axis) or time t (upper x-axis) for the PD induced by inhibitory autapse (olive) and for the DS in the absence of inhibitory autapse (orange).

3.2.5. DS for weak advance effect or delay effect of the inhibitory autapse

For the DS of $g_{\rm E} = 0.1$ μS/cm^2 and $\beta_{\rm E} = 0.3$ ms^{-1}, if an inhibitory autapse with weak advance effect [point C in Fig. 4(a), $g_{\rm I} = 1.6$ μS/cm^2 and $\beta_{\rm I} = 1$ ms^{-1}] is introduced, the behavior is still DS, as shown in Fig. 9. The weak advance effect of the inhibitory autapse cannot induce the i-th spike of neuron R to appear before the i-th spike of neuron S, but to advance to a small extent. Then, $\tau_i = t_i^{\rm R} - t_i^{\rm S}$ for the DS with inhibitory autapse (olive) converges to $\tau_{\rm s} \approx 0.517$ ms, which is shorter than $\tau_{\rm s} \approx 1.332$ ms (orange) for the DS in the absence of inhibitory autapse. In addition, if the inhibitory autapse with delay effect is introduced to the neuron R, it can be concluded that not the AS or PD but the DS appears. Such a condition is not shown here due to not the focus of this article.

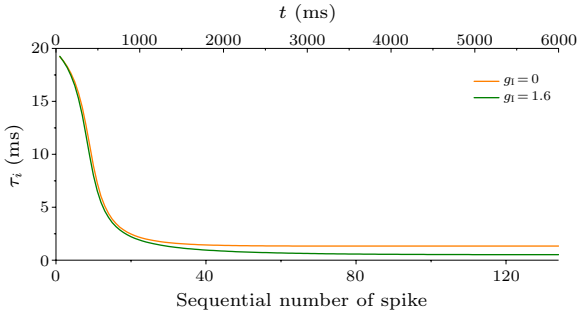


Fig. 9. Change of τ_i with respect to i (lower x-axis) or time t (upper x-axis) for the delayed synchronization (DS) with autapse (orange, $g_{\rm I} = 1.6$ μS/cm^2 and $\beta_{\rm I} = 1$ ms^{-1}) and in the absence of inhibitory autapse (olive).

3.3. Dependence of AS, PD, and DS on the inhibitory autapse and excitatory synapse

As mentioned above, the DS, AS, and PD behaviors are dependent on both the inhibitory autapse and excitatory synapse. The distributions of the DS, AS, and PD on the plane ($g_{\rm I}$, $\beta_{\rm I}$) at different $g_{\rm E}$ values and on the plane ($g_{\rm I}$, $\beta_{\rm E}$) at different values of $\beta_{\rm I}$ are addressed in the present subsection. It should be noticed that the delay effect of the excitatory synaptic current is stronger for a larger $g_{\rm E}$.

3.3.1. Dependence on the inhibitory autapse at different values of $g_{\rm E}$

The distributions of the AS (red), DS (green), and PD (yellow) on the plane ($g_{\rm I}$, $\beta_{\rm I}$) for $g_{\rm E} = 0.1$ μS/cm^2, 0.2 μS/cm^2,

0.3 μS/cm^2, 0.6 μS/cm^2, 1 μS/cm^2, and 1.5 μS/cm^2 are shown in Figs. 10(a)–10(f), respectively. Three characteristics can be found from Fig. 10.

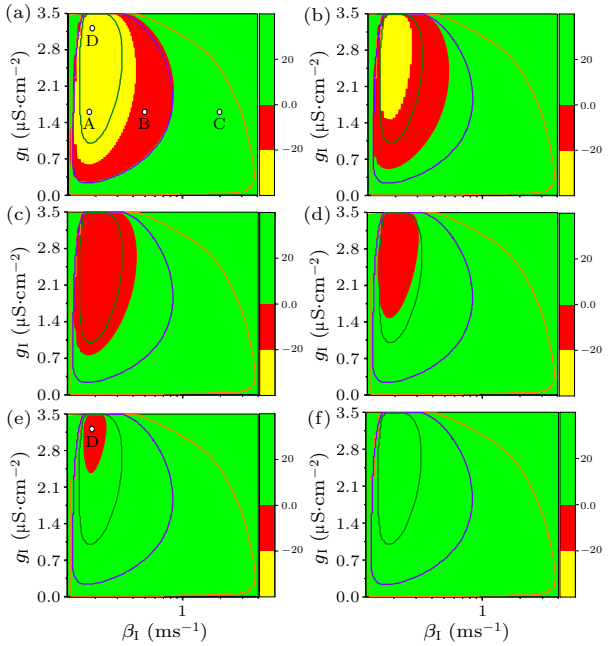


Fig. 10. Distributions of the DS (green), AS (red), and PD (yellow) on the plane (g_I, β_I) at different values of g_E for (a) $g_E = 0.1$ μS/cm^2, (b) $g_E = 0.2$ μS/cm^2, (c) $g_E = 0.3$ μS/cm^2, (d) $g_E = 0.6$ μS/cm^2, (e) $g_E = 1$ μS/cm^2, and (f) $g_E = 1.5$ μS/cm^2. Olive, violet, and orange curves represent the borders of the strong, middle, and weak advance effects of the inhibitory autapse, respectively.

(i) PD behavior (yellow) appears for small g_E [0.1 μS/cm^2 in Fig. 10(a) or 0.2 μS/cm^2 in Fig. 10(b)] and mainly within the region of (g_I, β_I) with strong advance effect (i.e., within the olive curve). Small g_E ensures that the delay effect of the excitatory synaptic current is small, and the strong advance effect of the inhibitory autapse ensures to overcome the delay effect of excitatory synaptic current. With increasing g_E, the delay effect of the excitatory synapse becomes stronger, resulting in the area for the PD becoming smaller, as shown in Figs. 10(a) and 10(b).

(ii) AS (red) mainly appears within the region of (g_I, β_I) with middle advance effect (i.e., within the violet curve) and for not strong g_E [Figs. 10(a)–10(e)]. The area of AS is outside of that of DS for small g_E and shrinks to be within the area of strong advances effect with increasing g_E. AS disappears for g_E larger than 0.1 μS/cm^2, as shown in Fig. 10(f).

(iii) The DS (green) appears in the remaining areas exclusive the AS and PD. The delay effect of the excitatory current is strong enough while the advance effect of the inhibitory autapse is relatively weak or not strong in the area of the DS. For example, as shown in Fig. 10(f) with large g_E, the delay effect of the excitatory synaptic current is strong enough to overcome the advance effect of the inhibitory autapse, resulting in DS in the whole plane (g_I, β_I). With decreasing g_E, the area of the DS becomes narrower, due to the decrease of the delay effect of the excitatory synaptic current.

3.3.2. Dependence of DS, AS, and PD on g_E and g_I for $\beta_I = 0.18$ ms^{-1}

To further identify the dependence of AS on g_I and g_E, the distribution of the AS (red), DS (green), and PD (yellow) in the plane (g_I, g_E) for $\beta_I = 0.18$ ms^{-1} is shown in Fig. 11(a). The AS and DS are denoted by the red and green, respectively, and the border between the red and green corresponds to $\tau_s = 0$ ms. The PD, AS, and DS behaviors appear in small, middle, and large g_E values, respectively. Within the PD region, g_I is much larger than g_E, showing that the inhibitory autapse plays a dominant role to advance the spike of the neuron R, compared with the delayed effect of the excitatory synaptic current. With increasing g_E, the range of g_I for PD reduces. Within the DS region with large g_E, showing that the delay effect of the excitatory synaptic current is dominant. Within the stable AS region with a middle g_E, the advance effect of the autaptic current and the delay effect of the synaptic current can realize a dynamic balance. With increasing g_E, the range of g_I for AS reduces, as shown in Fig. 11(b), i.e., the range of g_I for negative τ_s reduces.

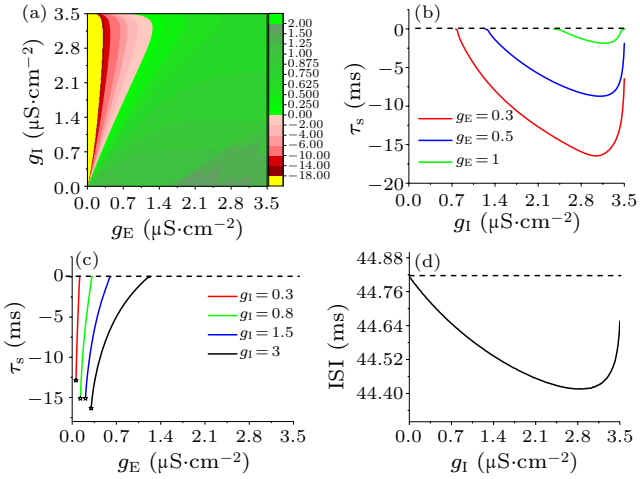


Fig. 11. Dependence of DS, AS, and PD on g_I and g_E for $\beta_I = 0.18$ ms^{-1}. (a) Distribution of DS (green), AS (red), and PD (yellow) in the parameter plane (g_I, g_E). (b) Changes of τ_s with respect to g_I at different values of g_E ($\tau_s < 0$ within the AS region). (c) Changes of τ_s with respect to g_E at different values of g_I ($\tau_s < 0$ within the AS region). (d) Changes of the ISIs with respect to g_I at $g_E = 0$ μS/cm^2.

3.3.3. Changes of τ_s of AS with respect to g_I or g_E

The changing trends of τ_s for the AS with increasing g_I at different g_E values, and with increasing g_E at different g_I values, are illustrated in Figs. 11(b) and 11(c), respectively, which exhibit three characteristics mainly determined by the advance effect of the inhibitory autapse [Fig. 4(c)] and the delay effect of the excitatory synaptic current. With increasing g_I, the advance effect of the inhibitory autapse for $\beta_I = 0.18$ ms^{-1} increases at first and then decreases, i.e., the ISI decreases firstly and then increases, as shown in Fig. 11(d) [for convenience to be compared with Figs. 11(a)–11(c)]. As g_E increases, the delay effect of the excitatory synaptic current becomes larger

[Fig. 2(c)]. Then, three characteristics are addressed as follows:

(i) With increasing g_I, g_E values of the border between AS and PD, the border between AS and DS, and the range of g_E for the AS, increase firstly and then decrease, exhibiting a changing trend similar to the advance effect of the inhibitory autapse, i.e., increases at first and then decreases with increasing g_I [Fig. 4(c)].

(ii) For a fixed g_E, the τ_s value for the AS decreases at first and then increases with increasing g_I, as illustrated in Figs. 11(a) and 11(b), which is mainly determined by the advance effect of the inhibitory autapse [Fig. 11(d)].

(iii) For a fixed g_I, the τ_s value increases with respect to the increase of g_E, as described in Fig. 11(c), due to the fact that the delay effect of the excitatory synaptic current becomes stronger.

3.3.4. Dependence of AS on g_I and g_E at different β_I values

The distributions of the DS, AS, and PD in the parameter plane (g_I, g_E) at different values of β_I ($\beta_I = 0.15$ ms^{-1}, 0.2 ms^{-1}, 0.4 ms^{-1}, 1 ms^{-1}) are shown in Figs. 12(a)–12(d), which can be explained by the advance effect of the inhibitory autapse shown in Figs. 4(a) and 4(c). As depicted in Fig. 4(c), at different β_I values, the advance effect of the inhibitory autapse increases firstly (from $\beta_I = 0.15$ ms^{-1} to 0.2 ms^{-1}) and then decreases gradually (from 0.2 ms^{-1} to 0.4 ms^{-1}, and to 1 ms^{-1}). Correspondingly, the areas of the AS and PD increase at first and then decrease, which is determined by the advance effect of the inhibitory autapse.

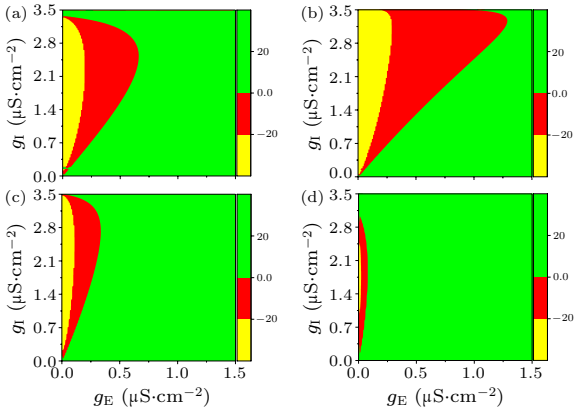


Fig. 12. Distributions of the DS (green), AS (red), and PD (yellow) on the parameter plane (g_I, g_E) at different values of g_I, for (a) $\beta_I = 0.15$ ms^{-1}, (b) $\beta_I = 0.2$ ms^{-1}, (c) $\beta_I = 0.4$ ms^{-1}, and (d) $\beta_I = 1$ ms^{-1}.

In summary, the inhibitory autaptic current plays a paradoxical role to advance the spike, which is the most important factor to induces AS and PD. If there is no the inhibitory autaptic current, AS or PD cannot be evoked. The excitatory synaptic current plays a paradoxical role to delay the spike, which is the most important factor to induce the DS.

4. Conclusions

Investigations in neurodynamics play important roles in at least two aspects. One is identification of complex and even counterintuitive phenomena in nonlinear dynamics. The other is identification of practical or potential functions of the nervous system. The anticipated synchronization (AS) of the nervous system exhibits significance in both aspects, such as the counterintuitive phenomenon that the response appears before the stimulation and the possible functions of coupled neurons or brain to anticipate the future or processing information.[17,18] Unfortunately, the dynamical or modulation mechanism for the AS remains unclear. In this paper, the dynamical mechanism for the AS modulated by an inhibitory autaptic current and an excitatory synaptic current is acquired, which is associated with the paradoxical roles of both the currents. The results exhibit significance in the following aspects.

Firstly, the dynamical mechanism for the AS is associated with a dynamic balance between the excitatory synaptic current and the inhibitory autaptic current, which presents deep understandings to the AS. The AS simulated in the sender-receiver neurons with an inhibitory autapse[18] is chosen as a representative studied in this article, due to the simple topology (two neurons) and less factors (no consideration of time delay). The inhibitory autaptic current plays a paradoxical role to advance the spike, which induces the spike of the receiver neuron to appear before the spike of the sender neuron. Then, the excitatory synaptic current plays a delay role to prevent the spike further advanced. The two currents exhibit opposite effects and realize a dynamic balance. Then, the comprehensive effect of two currents has no influence on the period of the spiking of the receiver neuron, resulting in the stable AS. The period of the spiking for the stable AS equals that of the single neuron without modulations. In conclusion, the advance effect of the inhibitory autaptic current, the delay effect of the excitatory synaptic current, and the dynamic balance between these two currents are the causes for the stable AS. In the previous studies,[33,60] synchronization transition of the bursting behaviors induced by the inhibitory modulations was explained with the dynamics of single neurons. In the present study, the dynamics of the anticipated synchronization is explained with the dynamic response of single neuron to the excitatory synaptic current and inhibitory autaptic current.

Secondly, the paradoxical roles of the excitatory stimulation/synaptic current and the inhibitory autaptic current are obtained, which present more examples of the counterintuitive phenomena of single neurons and enrich the contents of nonlinear dynamics. In the common viewpoint, the inhibitory autapse should induce spike activity reduced. However, in this article, the inhibitory autapse with suitable parameters (in a

range of conductance and decay rate) induce enhanced spiking activity (i.e., spike advances), which presents a novel paradoxical example that the inhibitory modulation can enhance firing activity and a novel potential function of the inhibitory autapse, other than those studied in the previous studies.[36,55] In general, the excitatory stimulation should enhance the firing activity. However, the excitatory stimulation with a suitable application phase can induce spiking with type-Ⅱ phase response curve reduced (i.e., spike delays). Such a result presents a paradoxical response of the Izhikevich model to the excitatory stimulation. The paradoxical roles of the inhibitory autaptic current and excitatory synaptic current extend the contents of nonlinear dynamics. In fact, in the remaining parameter region, the inhibitory autapse and the excitatory stimulation can play common roles. Then, the paradoxical or common roles of the inhibitory autapse and excitatory stimulation present comprehensive understandings to the complex modulations in single neurons.

Finally, the AS is compared with other dynamical behavior such as the PD and DS, which presents comprehensive understandings of the AS. For the AS, the advance effect of the inhibitory autapse and the delay effect of the synaptic current can realize a dynamic balance. Without the advance effect of the inhibitory autapse, AS cannot be evoked. As the advance effect of the inhibitory autapse is dominant to overcome the delay effect of the excitatory synaptic current, the PD behavior appears, i.e., the spike of the receiver neuron always advances. Such a recognition on PD is more detailed than that in Ref. [18], where the PD is described as a behavior with unstable interval between spikes of the sender and receiver neurons. The PD appears in the parameter region of the strong advance effect of the inhibitory autapse and the weak delay effect of the excitatory synaptic current, showing that the advance effect of inhibitory autapse plays a dominant role. As the advance effect of the inhibitory autapse is weak, or the delay effect of the excitatory synapse is strong, the spike of the receiver neuron cannot appear before the spike of the sender neuron, not the AS but the DS appears. Of course, in the absence of the inhibitory autapse, no advance effect modulates the spike of the receiver neuron advanced, resulting in the DS. Then, the advance effect of the inhibitory autapse is the necessary condition to evoke the AS. The conductances of the inhibitory autapse and excitatory synapse can be used as feasible measures to modulate the AS behavior and the transitions among the AS, PD, and DS.

Based on the results of the previous studies and this article, the dynamical mechanism for the AS appearing in other coupled systems with more neurons or modulations should be investigated in future. In the couple neurons or networks to simulate AS in different brain regions,[16–18,22,23] no time delay is considered. Then, the time lag between sender neurons and receiver neurons is from neural modulations. The inhibitory autapse of the receiver neuron considered in this article is an effective modulation measure to induce time lag of the AS. In addition, much attention should be paid to the paradoxical dynamics of single neurons to identify the dynamics of the counterintuitive AS. Considering that there is similarity between chemical autapse and memristor synapse,[61] the influences of the inhibitory memristor synapse on AS should be studied in future. Furthermore, more experimental studies to demonstrate the AS and to explore the functions of AS are expected.

Appendix A: The mathematical model of AS

The mathematical model of unidirectionally coupled sender and receiver systems is expressed as[3–5]

$$\frac{\mathrm{d}S}{\mathrm{d}t} = f(S(t)), \tag{A1}$$

$$\frac{\mathrm{d}S}{\mathrm{d}t} = f(R(t)) + KS(t). \tag{A2}$$

Equation (A1) corresponds to the sender system, where $S(t)$ is the system variable and $f(\cdot)$ defines the autonomous dynamical system. The $f(R(t))$ in Eq. (A2) corresponds to the receiver system, where $R(t)$ is the system variable. The coupled sender and receiver systems are identical. The second item of Eq. (A2) corresponds to the coupling or stimulation from the sender system to the receiver system, and K is the coupling strength or matrix. If a self-feedback delay regulation of the receiver system, $KR(t-t_\mathrm{s})$ (t_s represents the time delay), is introduced into the coupling item of Eq. (A2), then the coupled system becomes

$$\frac{\mathrm{d}S}{\mathrm{d}t} = f(S(t)), \tag{A3}$$

$$\frac{\mathrm{d}R}{\mathrm{d}t} = f(R(t)) + K[S(t) - R(t-t_\mathrm{s})]. \tag{A4}$$

If the coupled system of Eqs. (A3) and (A4) has the solution $R(t) = S(t+t_\mathrm{s})$ ($t_\mathrm{s} > 0$), it means that AS phenomenon occurs, due to the fact that the behavior $R(t)$ of the receiver system is identical to the behavior of S at the time $t+t_\mathrm{s}$ [i.e., $S(t+t_\mathrm{s})$] of the sender system. The result means that the behavior of the receiver system is transferred to the receiver system in advance, showing that the AS is a nonlinear counterintuitive behavior. The AS phenomenon has been verified in many theoretical and experimental studies, such as the experiment on unidirectionally coupled semiconductor lasers with delayed photoelectric feedback.

Appendix B: Simulation parameters

Table B1. Parameters to describe dynamics of single neuron and coupled neurons.

Variable	Parameter description
T_0	firing period of single neuron model without pulse stimulation
T_1	firing period of single neuron model with pulse stimulation
t_s	action moment of pulse stimulation
I_s	amplitude of pulse stimulation
D_s	duration of pulse stimulation
$\theta(t_s)$	$\theta(t_s) = (T_0 - T_1)/T_0$
t_i^R	the peak time of the i-th spike of the neuron R
t_i^S	the peak time of the i-th spike of the neuron S
τ_i	$\tau_i = t_i^R - t_i^S$
τ_s	if τ_i converges to a fixed constant value, labeled as τ_s

Acknowledgments

Project supported by the National Natural Science Foundation of China (Grant Nos. 12072236, 12162002, and 11802086), the Young Talents of Science and Technology in Universities of Inner Mongolia Autonomous Region (Grant No. NJYT-20-A09), and the Program for Excellent Young Talents in Colleges and Universities of Anhui Province of China (Grant No. gxyqZD2020077).

References

[1] Arenas A, Díaz-Guilera A, Kurths J, Moreno Y and Zhou C 2008 *Phys. Rep.* **469** 93
[2] Jiang M, Zhu J, Liu Y, Yang M, Tian C, Jiang S, Wang Y, Guo H, Wang K and Shu Y 2012 *PLoS Biol.* **10** e1001324
[3] Voss H U 2000 *Phys. Rev. E* **61** 5115
[4] Voss H U 2001 *Phys. Rev. Lett.* **87** 014102
[5] Voss H U 2016 *Phys. Rev. E* **93** 030201
[6] Wang H J, Huang H B and Qi G X 2005 *Phys. Rev. E* **71** 015202
[7] Li F, Hu A H and Xu Z Y 2006 *Chin. Phys.* **15** 507
[8] Ciszak M, Mirasso C R, Toral R and Calvo O 2009 *Phys. Rev. E* **79** 046203
[9] Mayol C, Mirasso C R and Toral R 2012 *Phys. Rev. E* **85** 056216
[10] Hayashi Y, Nasuto S J and Eberle H 2016 *Phys. Rev. E* **93** 052229
[11] Ciszak M, Calvo O, Masoller C, Mirasso C R and Toral R 2003 *Phys. Rev. Lett.* **90** 204102
[12] Pyragienė T and Pyragas K 2013 *Nonlinear Dyn.* **74** 297
[13] Sausedo-Solorio J M and Pisarchik A N 2014 *Phys. Lett. A* **378** 2108
[14] Washburn A, Kallen RW, Lamb M, Stepp N, Shockley K and Richardson M J 2019 *PLoS ONE* **14** e0221275
[15] Roman IR, Washburn A, Large EW, Chafe C and Fujioka T 2019 *PLoS Comput. Biol.* **15** e1007371
[16] Matias F S, Carelli P V, Mirasso C R and Copelli M 2011 *Phys. Rev. E* **84** 021922
[17] Matias F S, Gollo L L, Carelli P V, Bressler S L, Copelli M and Mirasso C R 2014 *NeuroImage* **99** 411
[18] Pinto M A, Rosso O A and Matias F S 2019 *Phys. Rev. E* **99** 062411
[19] Matias F S, Gollo L L, Carelli P V, Mirasso C R and Copelli M 2016 *Phys. Rev. E* **94** 042411
[20] Matias F S, Carelli P V, Mirasso C R, Mirasso C R and Copelli M 2017 *Phys. Rev. E* **95** 052410
[21] Dima G C, Copelli M and Mindlin G B 2018 *Int. J. Bifurcat. Chaos* **28** 1830025
[22] Dalla P L, Matias F S, Santos A J, Alonso A, Carelli P V, Copelli M and Mirasso C R 2019 *Front. Syst. Neurosci.* **13** 41
[23] Brito K V P and Matias F S 2021 *Phys. Rev. E* **103** 032415
[24] Machado J N and Matias F S 2020 *Phys. Rev. E* **102** 032412
[25] Salazar R F, Dotson N M, Bressler S L and Gray C M 2012 *Science* **338** 1097
[26] Brovelli A, Ding M, Ledberg A, Chen Y, Nakamura R and Bressler SL 2004 *Proc. Natl. Acad. Sci. USA* **101** 9849
[27] Mindlin G B 2017 *Chaos* **27** 092101
[28] Tass P, Kurths J, Rosenblum M G, Guasti G and Hefter H 1996 *Phys. Rev. E* **54** R2224
[29] Carlos F-L P, Ubirakitan M-M, Rodrigues M C A, Aguilar-Domingo M, Herrera-Gutiérrez E, Gómez-Amor J, Copelli M, Carelli P V and Matias F S 2020 *Phys. Rev. E* **102** 032216
[30] Dodla R and Rinzel J 2006 *Phys. Rev. E* **73** 010903
[31] Dodla R, Svirskis G and Rinzel J 2006 *J. Neurophysiol.* **95** 2664
[32] Winograd M, Destexhe A and Sanchez-vives M V 2008 *Proc. Natl. Acad. Sci. USA* **105** 7298
[33] Li Y Y, Gu H G, Jia B and Ding X L 2021 *Sci. China Technol. Sci.* **64** 1459
[34] Wang X, Gu H and Jia Y 2023 *Chaos Soliton Fract.* **166** 112904
[35] Wu F Q and Gu H G 2020 *Int. J. Bifurcat. Chaos* **30** 2030009
[36] Zhao Z G, Li L and Gu H G 2020 *Commun. Nonlinear Sci. Numer. Simulat.* **85** 105250
[37] Wang J, Xu J, Wu J and Xu Q 2022 *Cogn. Neurodyn.* **16** 1505
[38] Li L, Zhao Z and Gu H 2022 *Chin. Phys. B* **31** 070506
[39] Qi C S, Li Y Y, Gu H G and Yang Y X 2022 *Cogn. Neurodyn.* (online)
[40] Yang Y, Cui Y, Sang K, Dong Y Y, Ni Z Y, Ma S S and Hu H L 2018 *Nature* **554** 317
[41] Kim J, Kim Y, Nakajima R, Shin A, Jeong M, Park A H, Jeong Y, Jo S, Yang S, Park H, Cho S H, Cho K H, Shim I, Chung J H, Paik S B, Augustine G and Kim D 2017 *Neuron* **95** 1181
[42] Wang H T, Wang L F, Chen Y L and Chen Y 2014 *Chaos* **24** 033122
[43] Ding X L, Jia B and Li Y Y 2019 *Acta Phys. Sin.* **68** 080502 (in chinese)
[44] Wang H T and Chen Y 2015 *Chin. Phys. B* **24** 128709
[45] Yin L, Zheng R, Ke W, He Q,Zhang Y, Li J, Wang B, Mi Z, Long Y S, Rasch M J, Li T, Luan G and Shu Y 2018 *Nat. Commun.* **9** 4890
[46] He Z W, Yao C G, Shuai J W and Nakano T 2020 *Chin. Phys. B* **29** 128702
[47] Yilmaz E, Ozer M, Baysal V and Perc M 2016 *Sci. Rep.* **6** 30914
[48] Ma J, Song X, Jin W and Wang C 2015 *Chaos Soliton Fract.* **80** 31
[49] Yao C G, He Z W, Nakano T, Qian Y and Shuai J W 2019 *Nonlinear Dyn.* **97** 1425
[50] Sun X J and Si H 2020 *Nonlinear Dyn.* **100** 2673
[51] Yilmaz E, Baysal V, Perc M and Ozer M 2016 *Sci. China Technol. Sci.* **59** 364
[52] Jia Y B, Gu H G, Li Y Y and Ding X L 2021 *Commun. Nonlinear Sci. Numer. Simulat.* **95** 105643
[53] Jia Y B, Gu H G and Li Y Y 2022 *Cogn. Neurodynamics* (online)
[54] Bacci A, Huguenard J R and Prince D A 2003 *J. Neurosci.* **23** 859
[55] Tikidji-Hamburyan R A, Martinez J J, White J A and Canavier C C 2015 *J. Neurosci.* **35** 15682
[56] Xu Y and Ma J 2021 *Chin. Phys. B* **30** 100501
[57] Saada R, Miller N, Hurwitz I and Susswein A J 2009 *Curr. Biol.* **19** 479
[58] Guo D Q, Chen M M, Perc M, Wu S D, Xia C, Zhang Y S, Xu P, Xia Y and Yao D Z 2016 *Europhys. Lett.* **114** 30001
[59] Izhikevich E M 2003 *IEEE Trans. Neural Netw.* **14** 1569
[60] Belykh I and Shilnikov A 2008 *Phys. Rev. Lett.* **101** 078102
[61] Wu F, Gu H and Jia Y 2021 *Chaos Soliton Fract.* **153** 111611